

Nano-Silicon Sol-Gel Film Refraction Index Modulation with Femtosecond Laser

Antonela Dima^{1,a}, Massimo Gagliardi^{2,b}, Dun Liu^{1,c}, Walter Perrie^{1,d},
Craig J. Williams^{1,e}, Ivo Rendina^{2,f}, Geoff Dearden^{1,g}, Ken G. Watkins^{1,h}

1. The University of Liverpool (UOL), Brownlow Hill, Liverpool L69 3GH, United Kingdom
2. Istituto per la Microelettronica e Microsistemi (IMM-CNR), via P. Castellino 111, Napoli 80131, Italy

^a antonela.dima@liv.ac.uk, ^b Massimo.gagliardi@na.imm.cnr.it, ^c dun.liu@liv.ac.uk, ^e c.j.williams@liv.ac.uk, ^f ivo.rendina@na.imm.cnr.it, ^g g.dearden@liv.ac.uk, ^h k.watkins@liv.ac.uk

Keywords: silicon nanoparticles, sol-gel, waveguides, laser direct writing

Abstract: Patterned structures were created by exposing SiO₂ sol-gel films containing nano-silicon particles to a Clark MXR CPA-2010 fs laser (387 nm). A refractive index variation of 0.2 was obtained, similar to that of polymer films, however in an entirely superior stability class (structural, chemical, thermal, radiation, etc). The useful optical range of refractive index modulation is beyond 800 nm, respectively near-IR. Material characteristics were investigated with atomic force microscopy (AFM), Raman spectroscopy and spectro-ellipsometry measurements. Material properties were also investigated on different substrates in order to determine the influence of substrate type in laser processing.

Introduction

Direct laser writing techniques gained popularity in the last decade for a variety of applications, ranging from planar optical waveguides (needing no complex photolithographic processing) to material modulation. One of the techniques used is based on the focusing UV irradiation [1,2] onto Germania doped planar films deposited on silica – in order to gain a refractive index increase in the region exposed and form a “laser-written” waveguide. The refractive index modification forms the core of the waveguide, achieved refractive index changes being on the order of 10⁻³. Femto-second lasers [3–5] also cause change in the structure of the silica – in turn itself contributing to a refractive index increase, of the same order (~10⁻³). The modulation depends on exposure time, optical power and beam focusing. Erbium doped silica is a prime candidate for such techniques given its commercial availability and better properties for laser writing, permitting a relatively high modulation [6].

Separately from these investigations, the study of materials and devices containing nano-silicon crystals brought new devices with superior properties – such as intense light emission, making them potent candidates for Si-based opto-electronics. Such technological options are: nanoscale porous silicon (NPS), Si nanocrystalline embedded SiO₂ (SiO_x, $x < 2.0$) matrices (nc-Si/SiO₂), Si nanoquantum dots (SNQD) and Si/SiO₂ superlattices.

In this paper we present a SiO_x ($x < 2$) thin film containing nanocrystalline silicon particles. Patterning was obtained exposing the nc-Si/SiO₂ sol-gel film to a Clark MXR CPA-2010 fs laser (387 nm) for optical modulation. The refractive index changes and optical properties were monitored with spectro-ellipsometric analyses.

Experimental

Nano-Si/SiO₂ layers. The nc-Si/SiO₂ layers were deposited in sol-gel technology. The precursor for the SiO₂ solution was TEOS (TetraEthyl OrthoSilicate - Si(OC₂H₅)₄ from Sigma Aldrich). Ethanol was used as solvent. The solution containing silicon nanoparticles was added dropwise to

the TEOS solution. This solution was then filtered through an Acrodisc syringe filter of 200 nm porosity (Sigma Aldrich) and deposited by spin-coating (200 rpm for 20 s) on a silicon wafer. After spin-coating the wafers were dried in air at 100 °C. A final thermal treatment at 400 °C was performed, resulting in amorphous SiO₂ films embedding the Si nanoparticles. A higher temperature thermal treatment in air is not recommended as it can lead to the oxidation of the nc-Si particles during the heating.

The nano silicon particles added to the sol-gel solutions were obtained through smooth anisotropic etching in a tetramethylammonium hydroxide (TMAH) 20 % solution in methanol at 50 °C. Traditional etching in KOH is not suitable for Si particles due to contamination with potassium ions. According to Biswas et al. [7] the etching rate for the conditions stated is 4 μm/h. At this rate, given the average particle size, the approximate etching time is 5-15 min (hydrochloric acid added to pH = 3). This solution, with nc-Si but also with particles of bigger size, is mixed with the TEOS solution, the larger particles being filtered away. The size distribution of the remaining nc-particles is then 5 - 200 nm (filter pore size).

Laser modified nano-Si embedded in SiO₂ sol-gel layers.

The experiments were performed using a Clark-MXR CPA-2010 regenerative amplified Ti: sapphire laser system with a repetition rate of 1 KHz, pulse duration of 180 fs and a fundamental wavelength of 775 nm. UV 387 nm wavelength was produced by frequency doubling of the 775nm wavelength using a beta-BaB₂O₄ (BBO) crystal. The experimental setup is schematically shown in Fig. 1.

The beam diameter at the aperture of the laser system was 6mm. A high-energy variable diffractive attenuator was used for continuously adjusting pulse energy. The standard deviation in the pulse energy was ±1% of the average value. The nc-Si/SiO₂ film deposited on glass or on a silicon wafer is mounted on a computer controlled three axes stage (Aerotech). The beam was focused on the surface of the sample using a lens or an objective with different NAs. Pulse energies in the range of 0.5-1 μJ were used.

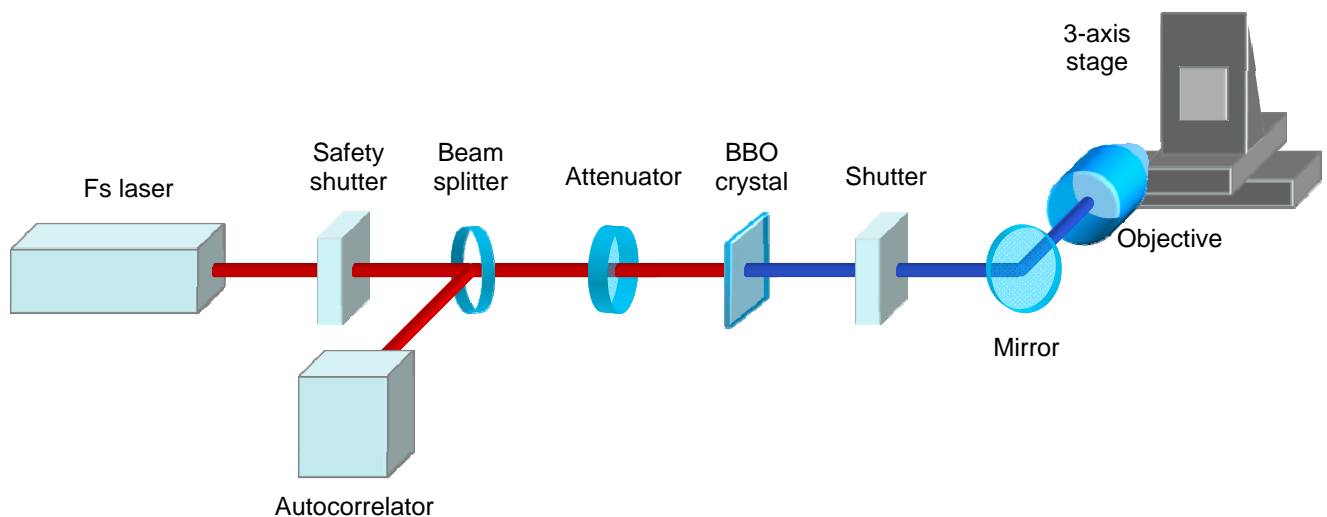


Fig 1 The experimental setup used for refractive index modulation using femtosecond UV laser technology.

Silica thin films on silicon and glass substrates were chosen for micro-machining as they are the most widely used structures in planar light-wave circuits. The typical modulation value of 10^{-3} can be dramatically increased due to nc-Si particles inclusion in the film. Buried waveguides were fabricated inside the partially thermally cured sol-gel film (Fig. 2). Irradiated films prepared by homogeneous irradiation of the surface were analyzed with spectro-ellipsometry. The laser-cured film depth is around 96 nm, starting from a sol-gel film with 100 nm thickness.

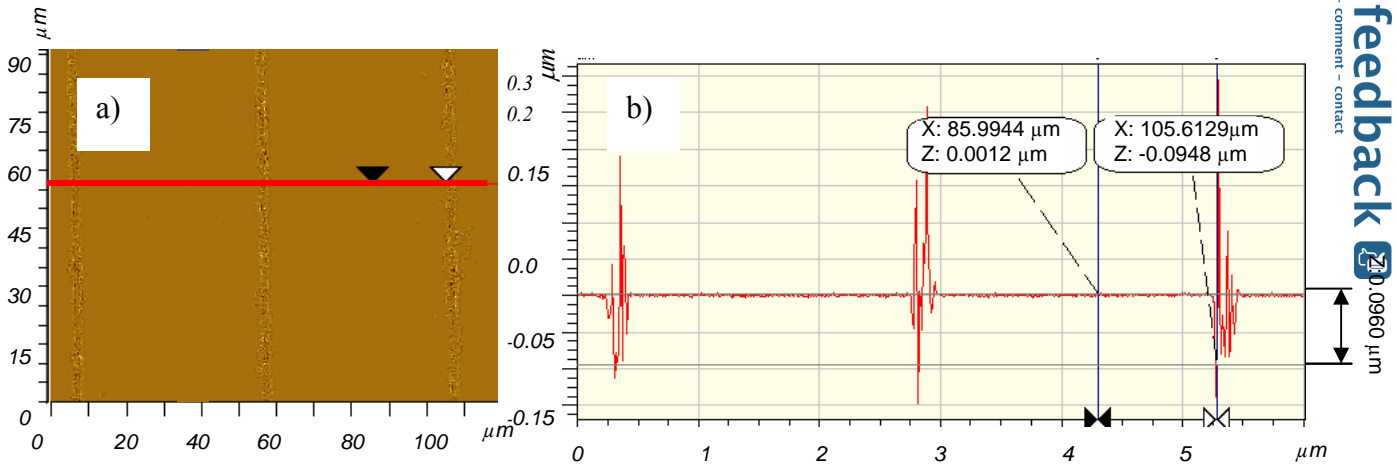


Fig 2 a) Buried waveguides fabricated using a 387 nm femtosecond laser on nc-Si/SiO₂ films deposited on silicon b) the optical profile of the surface

Results

AFM images were obtained using an Atomic Force Microscope (AFM) system with Veeco micromanipulation software. Fig. 3 shows the AFM image of the nano-silicon particles embedded into the SiO₂ sol-gel thin film. Nano-silicon clusters are present on the surface with varying sizes between 150-230 nm. The clusters are formed probably as a result of the spin coating process; however their presence is homogeneous on the surface.

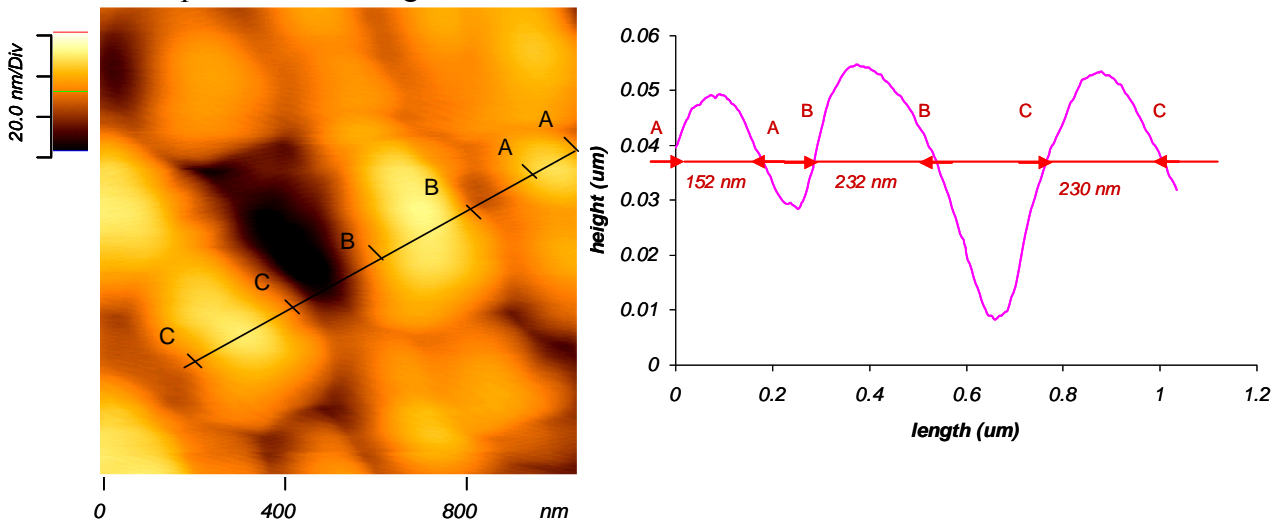


Fig 3 AFM images of a nc-Si/SiO₂ deposited on silicon wafer: clusters are seen at 20.0 nm/div with sizes between 150-230 nm

The polarized Raman spectra of the SiO₂ glass embedded with silicon nanoparticles were obtained with a high resolution Jobin-Yvon Horiba Raman confocal microscope using the 514.48 nm line of an Argon-ion laser as excitation source. The purpose of the measurement was to identify the nc-Si particles from the dried gel and to determine the effect of laser curing on the material. The experiment was performed on a nc-Si/SiO₂ dried gel (the drying performed in the air for a couple of weeks). In this way substrate influence is avoided, as well as that of oxidation of the nc-Si particles during thermal treatment (done with the purpose of removing organic residues from the thin film).

The spectral range investigated was 200–2000 cm⁻¹ and the beam was consistently focused on the virgin sol-gel glass and separately on the laser-cured surface. A number of bands in the Raman spectrum of the sol-gel glass (fig. 4) are identified as belonging to bulk vitreous silica. Hence, certain aspects of the vibrational structure of the nc-Si/SiO₂ gel already resemble those of fused silica.

The main feature of the spectrum of fused silica is the broad band centered at $\sim 440 \text{ cm}^{-1}$ (ω_1) previously attributed to the Si-O-Si bond rocking and bending in SiO_4 tetrahedra [8]. This appears in both sol-gel spectra (fig. 4). The peak intensity on the irradiated glass is higher due to the flash heating process and quenching of the amorphous silicon during the laser curing [9].

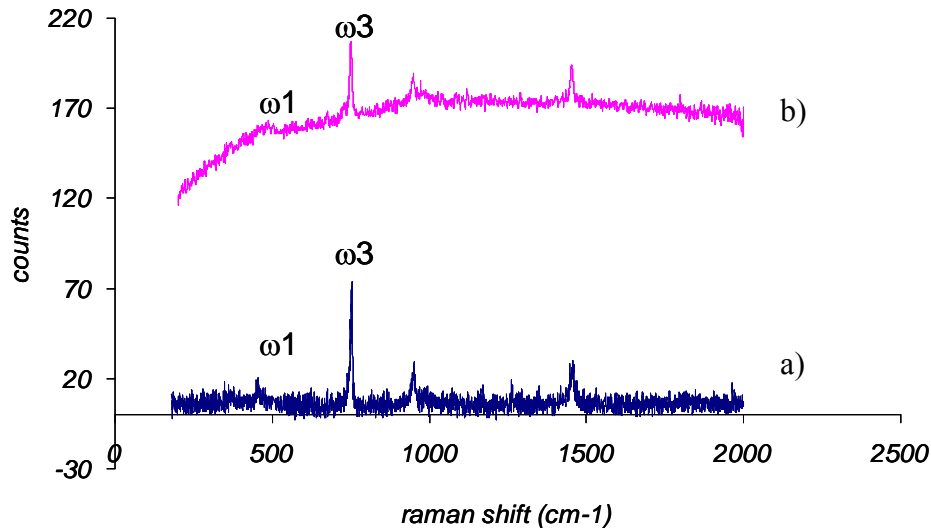


Fig 4 Raman spectrum of the a) unmodified nc-Si/SiO₂ gel and b) laser modified nc-Si/SiO₂ gel

The ω_3 peak is probably ascribed to a markedly broad overtone band centered at about 790 cm^{-1} attributed to the Si-O-Si symmetric stretching mode appears with high intensity in the uncured gel spectrum shifted at lower frequencies. The lower intensity of the peak in the cured gel case suggests changes into the silica glass structure during the laser curing with inclusion of nc-Si particles and new rearrangements into the network.

Other bands specific to the sol-gel spectra are observed at 950 cm^{-1} (typical of the Si-O stretching vibration of silanol (Si-OH) groups [10]) and at 1459 cm^{-1} (related with the CH_3 asym def [11]). We observe a progressive decrease of the intensity of the silanol band (Si-OH around 980 cm^{-1}) with respect to the intensity of the Si-O-Si band around 430 cm^{-1} . This corresponds to the condensation reaction between silanol groups to form the siloxane backbone. The silanol band is thus a very good indicator of the densification state of the gel [12]. It has been reported that the intensity of the Raman signal drops sharply when nc-Si concentration becomes less than 28 % and at the Si-poor end it is not detected, implying a sharp decrease in the number of silicon nanocrystallites [13], explaining thus why the 520 cm^{-1} peak specific to crystalline Si is absent in the sol-gel glass Raman spectrum.

The optical properties (complex refractive indexes), thickness and the anisotropy of the sol-gel material were determined from spectroellipsometric (SE) data analysis with the aim to model its non-linear behavior and investigate its intrinsic non-linear properties. SE measurements were performed by using a spectroscopic ellipsometer (Jobin Yvon, Model UVISEL NIR). Ellipsometric data was acquired at an angle of incidence of 45° in the range 350 – 1600 nm with a step of 5 nm. The SE spectra present (I_s , I_c) variables functions (fig 5a) of the (Ψ , Δ) ellipsometric angle measurements were I_s and I_c equation are given by:

$$I_s = \sin 2\Psi \sin \Delta$$

$$I_c = \sin 2\Psi \cos \Delta$$

A 3-layer model accurately describes the pristine nc-Si/SiO₂ film deposited on Si. The model takes into account the silicon substrate, a dense sol-gel SiO₂ film and a mixture of 50/50 void and film material. The optical model was described by the Tauc-Lorenz dispersion law in order to extract material characteristics. The film is highly transparent beyond 300 nm and adsorbent under 300 nm with a characteristic bandgap at 4 eV and a refractive index behavior similar to the one reported by

Chen et al [14]. The film is dense (a thin void layer of 5.95 nm being determined) with a thickness of approximately 100 nm.

The columnar structure of the laser-cured surface introduces uniaxial optical properties (optical axis perpendicular to the surface) similar to the one displayed by porous silicon [16]

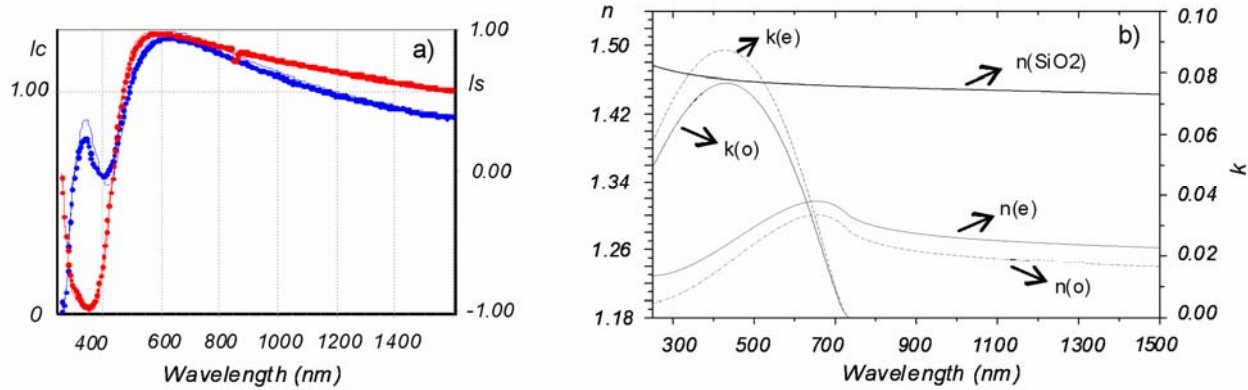


Fig 5 a) Ellipsometric data as (I_s , I_c), which relate to the ellipsometric angles Ψ and Δ ; and afferent model (described in the text) fitted to the data; b) refractive index and coefficient of extinction dependence on wavelength. The 300-1600 nm data show low birefringence with ordinary n_o and k_o (perpendicular to surface) and extraordinary n_e and k_e (within the surface). The $n(\text{SiO}_2)$ curve is for the pristine layer.

The 3-layer model (fig 5-a) takes into account the anisotropy of the structure determined by the silicon substrate and a mixture between 77 % SiO_2 and 23 % Si nanoparticles deposited on top of it. Fig. 5(b) shows the spectra of refractive indexes n_o and n_e – respectively extinction coefficients k_o and k_e , in the range from 300 to 1600 nm, as well as their difference, obtained from the best values of all parameters. The index dispersion is that typical for dielectric materials. The measured birefringence of nc-Si/ SiO_2 film is less than 0.031 in the whole UV–near IR range, respectively rather low. A positive birefringence is characteristic for the cured layer ($n_e - n_o > 0$) with the lower value close to 800 nm (corresponding to the highest value of the refractive index). In the extinction coefficient case the highest value corresponds to a maximum of absorption.

Table 1 Optical properties of laser-modified thin nc-Si/ SiO_2 films on silicon and glass substrate

Film type	nc-Si/ SiO_2 sol-gel film on Si				nc-Si/ SiO_2 sol-gel film on glass			
	Thickness [nm]	n at 300 nm	n at 1500 nm	Optical bandgap	Thickness [nm]	n at 300 nm	n at 1500 nm	bandgap
Virgin sol-gel film	100	1.524	1.488	4	220	1.468	1.445	3.26
Laser cured sol-gel film	137	1.23	1.27	1.5	220	1.485	1.42	1.2
Refractive index change		0.294	0.218			-0.017	0.025	

The determined thickness for the cured film is 137 nm. The cured film is absorbent under 800 nm and the determined optical bandgap is 1.5 eV (table 1). The absorbent properties of the silicon substrate at the laser wavelength could influence the properties of the laser cured film (possible substrate melting with subsequent diffusion through the sol-gel layer). In this case, a thicker film was deposited on a glass substrate and the same experiment was performed. The refractive index change is lower but the optical bandgap is still the same (table 1) displaying a value closer to silicon bandgap. This change is possible if rearrangement inside the silica network takes place and Si nanoparticles become a part of the silica network (as concluded also by Raman measurements).

Conclusions

The patterned structures created by exposing a SiO₂ sol-gel film containing nano-silicon particles to a Clark MXR CPA-2010 fs laser (387 nm) display a very high refractive index variation (0.2 for silicon substrates, respectively 0.02 for glass substrates). The useful optical range of refractive index modulation is beyond 800 nm, respectively near-IR. The utility of the films is also below 800 nm – as absorbers, case in which the un-cured parts are VIS-transparent, while the laser-cured ones opaque. Applications of stated properties are holographic plates, optical isolators, etc, with a potential high-tech niche in phase matching for Mach-Zehnder interferometers in ultra-fast light pulse modulation applications – where active modulating elements cause static unbalance of the interferometer setup. Balancing the interferometer via electrical bias of the active elements reduces the available dynamic range of the modulator, hence a precise phase matching element in the optical circuit is very useful – especially one that can be produced without further material deposition, directly through irradiation. The optical transparency of the laser-cured material decreases drastically in visible (up to 600 nm) due to the 1.5 eV bandgap. This onset is correlated with the formation of a cured glassy phase (revealed by Raman spectroscopy) uniaxial optically (determined ellipsometrically). The synthesis of laser-modified structures with a strong periodic modulation of refractive indices of the alternating structures was been developed with success. It is interesting to note that the pristine films display a moderately wide bandgap (3.87 eV), contrasting with that of the laser-cured ones – which can be useful in holographic and perhaps photovoltaic applications.

Acknowledgments

This research was carried out under the support of the EU Commission Grant MTKD-CT-2004-517165.

References

- [1] J. Hubner, C.V. Poulsen, J.E. Pedersen Mogens, R. Poulsen, T. Feuchter, M. Kristensen, Proc. SPIE. 2695 (1996) 98.
- [2] C. B. E. Gawith, G. D. Emmerson, S. P. Watts, V. Albani, M. Ibsen, R. B. Williams, P. G. R. Smith, S. G. McMeekin, J. R. Bonar, R. I. Laming, Lasers and Electro-Optics Europe 2003, CLEO/Europe 2003 Conference on 22–27 June 2003, p. 511.
- [3] S. Nolte, M. Will, J. Burghoff, A. Tunnermann, J. Mod. Opt. **51** (2004) 16.
- [4] J.W. Chan, T.R. Huser, S.H. Risbud, J.S. Hayden, D.M. Kroll, Appl. Phys. Lett. **82**(2003) 15.
- [5] A. Salimonia, N.T. Nguyen, M.-C. Nadeau, S. Petit, S.L. Chin, R. Vallee, J. Appl. Phys. **93** (2003) 7.
- [6] Yigang Li, Zian He, Hengsheng Tang, Liying Liu, Lei Xu, Wencheng Wang, Journal of Non-Crystalline Solids **354** (2008) 1216
- [7] K. Biswas, S. Kal, Microelectronics Journal, 37 (2006) 519-525
- [8] F.L. Galeener, A.E. Geissberger, Phys. Rev. B **27** (1983) 6199
- [9] K. Awazu, Journal of Non-Crystalline Solids **337** (2004) 241–253
- [10] E.I. Kamitsos, A.P. Patsis, Phys. Rev. B **48** (1993) 12 499
- [11] Ying-Sing Li, Abdul Ba, Spectrochimica Acta Part A **70** (2008) 1013
- [12] J.M. Nedelec, L. Courtheoux, et al., J Sol-Gel Sci Technol 46 (2008) 259
- [13] T.V. Torchynska, A. Vivas Hernandez, Y. Goldstein, J. Jdrzejewskii, S. Jimenez Sandoval, Journal of Non-Crystalline Solids **352** (2006) 1152
- [14] T.P. Chen, Y. Liu, M.S. Tse, O.K. Tan, P.F. Ho, K.Y. Liu, Phys. Rev. B **68**, 153301 (2003)
- [15] A. Tanaka, R. Saito, T. Kamikake, M. Imamura, H. Yasuda, Eur. Phys. J. D **43** (2007) 229
- [16] M. Gaillet, M. Guendouz, M. Ben Salah, B. Le Jeune, G. Le Brun, Thin Solid Films, **455-456**(2004) 410

Smart Materials for Smart Devices and Structures

doi:10.4028/3-908454-52-2

Nano-Silicon Sol-Gel Film Refraction Index Modulation with Femtosecond Laser

doi:10.4028/3-908454-52-2.101